Internet Appendix for "Quantifying Reduced-Form Evidence on Collateral Constraints"

SYLVIAN CATHERINE, THOMAS CHANEY, ZONGBO HUANG,

DAVID SRAER and DAVID THESMAR [1]

ABSTRACT

This appendix contains:

- a detailed literature review of structural / quantitative papers assessing the role of financial frictions (Section I);
- the method used to solve and estimate the model (Section II);
- the methodology used to solve and estimate 4,000 alternative models in our exploration of misspecification (Section III);
- additional comparative static results in partial equilibrium designed to show that the model is well behaved around the estimate (Figures IA1 to IA5);
- a description of the various adjustments to debt, total assets, physical capital, and investment that we use when we explore potential misspecification due to measurement issues in Section V of the main article (Section IV).

[1]Citation format: Catherine, Sylvian, Thomas Chaney, Zongbo Huang, David Sraer, and David Thesmar, Internet Appendix for "Quantifying Reduced-Form Evidence on Collateral Constraints," *Journal of Finance*, DOI: 10.1111/jofi.13158. Please note: Wiley-Blackwell is not responsible for the content or functionality of any additional information provided by the authors. Any queries (other than missing material) should be directed to the authors of the article.

I. Detailed Literature Review

We first review the quantitative macroeconomic literature on financial frictions, with an emphasis on the moments targeted in the estimation / calibration. A first strand of this literature relies on aggregate data. Kahn and Thomas (2013) consider state-dependent collateral constraints: constraints in the normal state are calibrated by targeting a debt-to-asset ratio of 0.372 in the nonfarm nonfinancial sector using data from the Flow of Funds; constraints in the bad state are set to match a 26% drop in debt in crisis times. Liu, Wang, and Zha (2013) focus, like us, on fluctuations on house prices and their effect on investment. They calibrate the steady-state level of collateral constraint by matching a debt-to-asset ratio of 0.75 for nonfarm nonfinancial corporate businesses and nonfarm noncorporate businesses.[2] Bernanke, Gertler, and Gilchrist (1999) develop a dynamic general equilibrium model to quantify the role of credit market frictions in business fluctuations; their calibration sets bankruptcy costs to match, in particular, an aggregate debt-to-physical capital ratio of 0.5. Jo and Senga (2019) study the aggregate impact of targeted credit subsidies in a heterogeneous firm model with collateral constraints and endogenous entry and exit. The parameter value in the collateral constraint is set to match the average debt-to-capital ratio of 0.57 for the nonfarm, nonfinancial businesses in the Flow of Funds from 1954 to 2007. While these papers target an aggregate debt-to-capital ratios, other papers normalize the aggregate stock of debt or external finance with output.

Midrigan and Xu (2014) evaluates the importance of financial constraints for misallocation by matching the aggregate debt-to-output ratio in Korea of 1.2. In their quantitative analysis of the role of financial frictions for development dynamics, Buera and Shin (2013) set the collateral constraint to match a cross-country average external finance-to-GDP ratios of 0.6. Moll (2014) adopts a similar approach to calibration: collateral constraints are set to match an average external-

[2]To obtain this ratio, they measure business debt as the sum of all credit market instrument and assets as the value of commercial land and equipment and software.

finance-to-GDP ratio for India of 0.54. In a similar vain, Itskhoki and Moll (2019) select a collateral constraint parameter to match an external finance to GDP ratio of 2.3. Jermann and Quadrini (2012) offer a quantitative exploration of how the dynamics of real and financial variables are affected by "financial shocks"; they calibrate the collateral constraint parameter to a steady-state ratio of debt over quarterly output of 3.36.

Finally, two notable contributions use aggregate data but focus on different variables for calibration purposes. Amaral and Quintin (2010) consider a model of economic development in which firms face a borrowing constraint. The extent of financial frictions is calibrated together with the degree of managerial talent by matching the ratio of intermediated capital to GDP and two moments of the labor size distribution of manufacturing establishments in the United States. Greenwood, Sanchez, and Wang (2013) also use aggregate data, but exploit a different moment. They quantify the impact of financial development on economic development using a costly state verification model of financial intermediation. The monitoring cost, which drives the extent of financial constraints in the model, is estimated by targeting an intermediation spread of 2.62% in the U.S. for 2004, calculated using NIPA data.

Another strand of the literature rely instead on firm-level data for calibration purposes. Cooley and Quadrini (2001) explain the simultaneous dependence of firm dynamics on size and age by introducing persistent shocks and financial frictions in a model of firm dynamics. The calibration is set in part to match the average leverage ratio of 0.25 documented in Hall et al. (1993) for Compustat firms. In Arellano, Bai, and Zhang (2012), the effect of financial development on firm dynamics is obtained by targeting an average leverage ratio among Bulgarian private firms of 0.36.[3] Gopinath et al. (2017) show how the decline in the real interest rate following the Euro convergence process leads to a significant decline in sectoral

[3]The estimation also matches the standard deviation of leverage and the mean leverage ratio for entrants.

total factor productivity due to financial frictions. They calibrate a size-dependent collateral constraint by targeting two moments: i) the fraction of firms that borrow to 0.90, and ii) the cross-sectional regression coefficient of firm leverage on log capital, which equals 0.15 in their data. Ottonello and Winberry (2020) quantitatively estimates the role of financial frictions and firm heterogeneity in the transmission of monetary policy to corporate investment. Their estimation targets an average firm-level gross leverage ratio of 0.34 from the microdata underlying the Quarterly Financial Reports. Their results suggest that lenders can recover 54% of the capital stock in bankruptcy. Garcia-Macia (2017) builds a model with heterogeneous firms that can invest in both physical and intangible capital and where intangible assets are harder to seize by creditors upon default. The model calibrates the collateral constraint on physical capital by targeting an average leverage ratio of 0.18 among private firms in Spain, as well as a cross-sectional regression coefficient of average investment ratio on leverage ratio. Finally, Gilchrist, Sim, and Zakrajšek (2014) evaluate the relative importance of financial frictions and uncertainty through the lens of a quantitative general equilibrium model. Bankruptcy costs, which characterize the degree of frictions in the bond market, are estimated to generate an average credit spread of 160 bps, which corresponds to the median of the BBB-Treasury spread. They find that about 10% of asset value is dissipated in the bankruptcy process.

The structural corporate finance literature also commonly targets the average leverage ratio to estimate the importance of financial frictions. Hennessy and Whited (2005) estimate a dynamic trade-off model with endogenous financing and investment against the predictions of a static trade-off model. Their model is estimated using SMM, and the estimation targets in particular an average net-debt-to-total-assets ratio of 0.075. They estimate a collateral constraint parameter of 0.59. Gomes and Schmid (2010) analyze the relation between leverage and stock returns in a structural dynamic model where both corporate investment and financing decisions are endogenous. Their model assumes that lenders can recoup

75% of asset values in bankruptcy, and it matches an average debt-to-total-assets ratio of 0.67. Hennessy and Whited (2007) infer the magnitude of financing costs by matching several moments related to corporate financing. In particular, they target an average net-debt-to-asset ratio of 0.12 on Compustat firms and estimate that about 10% of the capital stock is dissipated in default. DeAngelo, DeAngelo, and Whited (2011) estimate a dynamic capital structure model in which firms sometimes issue transitory debt and deviate deliberately, but temporarily, from leverage target in order to fund investment. Among other moments, they target an average leverage ratio of 0.24 (and its variance of 0.011). Their model does not include a collateral constraint; instead, it features an exogenous debt ceiling, which is estimated to be 72% of the steady-state capital stock. Li, Whited, and Wu (2016) consider the effect of taxes on leverage; they target an average debt-to-total-assets ratio of 0.29 in Compustat data and estimate a collateral constraint parameter that ranges from 0.37 to 0.46 depending on the tax rate. Begenau and Salomao (2018) explain cyclical patterns in corporate financing using a quantitative model with endogenous firm dynamics and financing frictions. Their calibrated model matches an average leverage ratio of 0.23 in Compustat by setting bankruptcy costs to 10% of total asset value and equity issuance costs of 20%. Michaels, Beau, and Whited (2018) explain the negative correlation of wages and leverage in a model that integrates factor adjustment frictions and wage bargaining with costly external financing. They target an average net-debt-to-total asset ratio of 0.35 and estimate that about 50% of the capital stock can be surrendered to the lender in default as collateral. Nikolov, Schmid, and Steri (2019) analyze quantitatively the role of credit lines in corporate liquidity management by developing a model where credit lines provide firms with financial flexibility, but are costly in terms of collateral. In the estimation, the collateral constraint parameter is set to match the average credit line limit of 17.2% along with an average leverage ratio (net of credit line) of 0.17 using Compustat data. The estimated collateral parameter is 0.33.

II. Solving the Model and Estimation

This section details the algorithms used to solve the model and estimate it. To estimate the model, one needs to find the set of parameters such that model-generated moments fit a pre-determined set of data moments. Because our model does not have an analytic solution, we need to use indirect inference to perform the estimation. Such inference is done in two steps:

- For a given set of parameters, we need to solve the model numerically, which means solving the Bellman problem (7) and obtain the policy function $S_{t+1} = (d_{t+1}, k_{t+1})$ as a function of $S_t = (d_t, k_t)$ and exogenous variables $X_t = (z_t, p_t)$.
- We then use this resolution technique to estimate the parameters that match best a set of moments chosen from the data. We explain the methodology (Simulated Method of Moments) and the numerical algorithm that we use to implement it.

A. *Solving the Model Numerically*

In this section, we describe how we numerically solve the firm's problem with given parameters.

A.1. Grid Definition

To solve the model numerically, we need to discretize the state space $(S; X)$. Let us start with the two exogenous variables. The log productivity process z is discretized using the standard Tauchen method on 51 grid points. Log real estate prices are also an AR(1), discretized using the Tauchen method on 11 grid points. For both variables, we set the bounds of the grid at -2.5 and 2.5 standard deviations.

Capital choice is discretized over a range from k_{min} to k_{max}, where k_{min} is the smallest level of capital chosen by a firm without adjustment costs and financing constraints. For this particular case, we can solve the capital decision analytically.

In most cases, this number should serve as a lower bound because adjustment costs would prevent firms from adjusting all the way down to this level; and financial constraints would push them to keep more capital as precautionary savings. Since we did not, however, establish this result analytically, we check that k_{min} is always "far enough" from the lowest simulated value of capital. Similarly, k_{max} is the capital stock chosen by unconstrained firms, without adjustment cost, facing the highest productivity level on the grid. Again, we expect this level to be above the upper bound of capital for a constrained firm with adjustment costs. We check that this is the case in our simulations. We then form an equally spaced grid for $\log$ capital between $\log k_{min}$ and $\log k_{max}$, with increment of $\log(1+\delta/2)$. Thus, the capital grid is geometrically spaced using $(1+\delta/2)$ as the multiplying coefficient, that is, the nth point is equal to $k_{min} \times (1+\delta/2)^n$ until k_{max}. Given that k_{min} and k_{max} are functions of productivity, the grid thus depends on the persistence ρ and volatility σ of log productivity. Larger persistence or volatility leads to a wider grid. In our preferred specification, capital evolves on a grid containing 270 points. We take this number as a reference when we discuss grid size below, bearing in mind that the capital grid is a function of parameter values.

Finally, the debt grid d_t is defined as a function of the amount of capital k_t. This adaptive feature of the debt grid comes from the fact that the amount of debt is bounded above by a function of capital: larger firms can borrow more. We restrict future-period debt d' to the $\left[-4\bar{d}; \bar{d}\right]$ interval, where $\bar{d} = s\left((1-\delta)k + p_{max}h\right)$ and p_{max} is the maximum house price level. The grid interval is thus a function of the model parameters s but also ρ and σ via the grid of k. The upper bound is a natural consequence of the collateral constraint: the model imposes that it cannot be exceeded. The lower bound is somewhat arbitrary as in theory there is no upper bound as to how much cash the firm may decide to hold. We check that there is no accumulation of cash at this bound during the estimation process. Within this interval, the grid is geometrically spaced so that it is denser when debt becomes closer to the constraint, that is, right below $\bar{d}$. We implement this by setting the

nth grid point to $\bar{d}\,(1 - 0.001 \times e^{.3n})$ until it reaches $-4\bar{d}$. Thus, the grid size for debt does not depend on parameters (in contrast to the capital grid size) and always has 29 points.

A.2. Bellman Resolution Algorithm

We solve the firm's problem using policy iteration. This algorithm is based on the fact that the value function is the solution of a fixed point problem generated by a contraction mapping.

Before starting to iterate, we compute profit flows $e(S, S'; X)$ using the production and cost functions, for all possible values of S and X on the grid. We set e to "missing" when $(S, S'; X)$ are such that $e < 0$ – the no equity issuance constraint is violated, or when the borrowing constraint is violated. Profits are only defined when both financing constraints are satisfied.

To initiate the process, we start with the value function $V_0\,(S; X) = 1$. We then look for the policy function $(k'_0, d'_0) = P_0(S; X)$ that solves

$$P_0(S; X) = \textbf{argmax}_{S'}\{e(S, S'; X) + \frac{1}{1+r}\} \tag{IA1}$$

for each state of $(S; X)$. Next, we iterate the following loop (where $n \geq 1$ denotes the step in the loop):

1. Start from $(k'_{n-1}, d'_{n-1}) = P_{n-1}(S; X)$, the policy function obtained from the previous round, and $V_{n-1}\,(S; X)$, the value function obtained from the previous round. For every point $(S; X)$ on the grid, we compute the value function V_n that satisfies:

$$V_n(S; X) = e(S, P_{n-1}(S; X); X) + \frac{1-d}{1+r}\mathbb{E}_{X'}\left[V_{n-1}(P_{n-1}(S; X'); X')|X\right] + \frac{d}{1+r}\left(k'_{n-1} - (1 + \tilde{r}_t)d'_{n-1}\right). \tag{IA2}$$

2. We then use the new value function V_n and compute the optimal policy given

this value function $(P_n(S;X))$:

$$P_n(S;X) = \textbf{argmax}_{S'}\{e(S,S';X) + \frac{1-d}{1+r}\mathbb{E}_{X'}\left[V_n(S';X')|X'\right] + \frac{d}{1+r}\left(k' - (1+\tilde{r}_t)d'\right)\}. \quad \textbf{(IA3)}$$

3. We stop when $P_n = P_{n-1}$.

Thanks to the contraction mapping theorem, we are guaranteed to find a good approximation of the value function $V(S;X)$ and the policy function $S' = P(S;X)$ defined over the grid. The computationally costly step is the determination of the policy function in step 2 with respect to S'. This consists of $29 \times 270 \times 51 \times 11 = 4,392,630$ optimizations of vectors with $29 \times 270 = 7,830$ points. This is where parallelization achieved through a GPU accelerates the process. For the range of parameters we explore, we typically solve the model in about two minutes with a GPU (Nvidia K80), compared to several hours with a CPU. What prevents us from having a finer grid is the RAM of the GPU, since the computer needs to create the maximand in step 2, a $29 \times 270 \times 29 \times 270 \times 51 \times 11 \approx 34$ billion numbers array.

The above algorithm is the standard policy function iteration algorithm. We make two adjustments to adapt it to our setting. First, to reduce computing time, we first solve the model with a coarser grid and then solve it again on the grid described above. To define this coarser grid, we divide the resolution of the control (k and d) grids by two. This divides computing time by four in the first step but only gives us the value and policy functions on the coarser grid. We then re-run the algorithm on the finer grid with the "coarser" policy and value functions as a starting point. Convergence occurs much more quickly.

The other adjustment is related to the treatment of missing values, which in our set-up occur when one of the two financing constraints is violated (i.e., the no-equity constraint or the collateral constraint). Without modification, the policy iteration algorithm does not behave well in the presence of missing values. This is because, for some given value functions V_{n-1}, there may exist some (S,X) for which

there is no acceptable policy S'. In this case, the optimal policy function $P_n(S, X)$ is not defined everywhere on the grid (note (S_0, X_0) such states for which the policy is not defined). When this happens, the next iteration value $V_n(S; X)$ is not defined for all (S, X), which leads with nonzero probability to states (S_0, X_0). As we iterate, missing values progressively spread to the entire grid and the algorithm is blocked. To solve this problem, we modify step 1 of the algorithm by requiring that $V_n(S; X)$ replaces $V_{n-1}(S; X)$ if and only if $V_n(S; X)$ is nonmissing. This prevents missing values from spreading to the entire grid of states $(S; X)$.

B. Estimation

We now estimate the parameters (s, c, ρ, σ, e) for which the model best matches a pre-defined set of moments (we experiment with a different set of moments and models in the main text).

B.1. Estimation Method: SMM

We estimate the key parameters of the model by simulated method of moments (SMM), which minimizes the distance between moments from real data and simulated data. Let us call m the vector of moments computed from the actual data, and Ω the moments generated by the model with parameters Ω. The SMM procedure searches the set of parameters that minimizes the weighted deviations between the actual and simulated moments,

$$\left(m - \widehat{m}\left(\Omega\right)\right)' W \left(m - \widehat{m}\left(\Omega\right)\right) \tag{IA4}$$

We detail the various components of our implementation in the following sections.

B.2. Empirical Moments m and Weight Matrix W

The empirical moments are computed in a simple way, and the definitions are given in the main text, in Section III.

The weight matrix W adjusts for the fact that some moments are more precisely estimated than others. It is computed as the inverse of the variance-covariance matrix of actual moments estimated by bootstrap with replacement on the actual data. To compute the elements of this matrix, we repeat 100 times the following procedure. Using our data set, we draw, with replacement, N firms with their entire history where N is the number of firms in the sample (we use the bsample command in Stata, clustered at the firm level). We then compute the moments and store them. Once we have performed this procedure 100 times, we compute the empirical variance-covariance matrix of the moments and invert it.

B.3. Model-Generated Moments m

Once we have solved the model for a given set of parameter Ω (Section II.A in the Internet Appendix), we need to simulate data in order to compute the simulated moments. We simulate a balanced panel of 1,000,000 firms over 100 years, and only keep the last 10 years to ensure each firm has reached steady-state. For each firm, we simulate a path of log productivities z_{it} and a path of log real estate prices p_{it}. This makes the variability of real estate prices larger than in the data, where prices only vary at the MSA level. Recall however that our objective in this simulation is not to replicate the variability of the data, but ideally to estimate model-generated moments. If we had closed forms for the model, we could measure these moments without infinite precision. The problem here comes from the fact that we cannot directly compute these moments but have to "estimate" them. Ideally, we would want to generate an infinitely large simulated dataset in order to compute the model-generated moments exactly, but computational constraints make it infeasible. 1,000,000 firms over 100 years already generate arrays with 100m entries. Allowing real estate prices to vary at the firm-level is a way to make sure the sensitivity to prices model-generated moments are estimated as well as possible.

B.4. Optimization Algorithm

We now have all the ingredients necessary to compute the objective function (IA4). In this section, we explain how to minimize it. Since in our most preferred specification we have five parameters, we need to make sure that we are indeed reaching a global minimum. We do this by implementing the following two-step procedure, which follows Guvenen, Ozkan, and Song (2014):

- We generate 1,000 quasi-random vectors of parameters Ω taken from a Halton sequence. The Halton sequence is a deterministic sequence of numbers that has the property of covering the parameter space evenly. For each of these parameters, we solve the model to obtain the policy function, simulate a dataset, compute the moments, and obtain the distance to data moments (IA4).

- We then use the lowest points (in terms of the objective function) as starting points for minimization. We iterate on the following loop. We begin with parameter estimate $\hat{\Omega}_1$ for which the objective function is the lowest. We then use the Nelder-Mead method (command *fminsearch* in Matlab) to perform local optimization starting from this point. We next compute the objective function O_1. We then move to the second-lowest parameter estimate ($\hat{\Omega}_2$) and compute the objective function O_2. We iterate on this and stop as soon as $O_n = 0$. Among the lowest parameters, a large fraction typically leads to the same parameters for which the objective function is equal to zero. This gives an indication that our objective function is well behaved.

There are no general theoretical results arguing that this technique dominates other popular algorithms adapted for large dimension optimization. In our setting, however, we found that the genetic algorithm and simulated annealing were much slower at converging. Also, this approach allows to "control" the smoothness of the objective function. For instance, within the lowest 20 parameters isolated after step 1, it would be worrisome if minimizations starting from each of these

parameters gave inconsistent parameters. On the contrary, they tend to be very consistent. The only cases in which convergence goes to the alternative choice of parameters than the one we present are cases where the objective function is much bigger than zero (i.e., other local optima). Finally, the best argument in favor of our selected estimates is the well-behaved comparative statics we present in Internet Appendix Figures IA1 to IA5.

B.5. Standard Errors

To compute standard errors, we use the standard formula for the variance-covariance matrix of parameter estimates $\hat{\Omega}$ in SMM estimation

$$\left(J'W^{-1}J\right)^{-1} + \left(J'\tilde{W}^{-1}J\right)^{-1},$$

which consists of two terms. The first term corresponds to the error coming from the estimation of data moments, where W is the variance-covariance matrix of data moments (which we use as weighting matrix in our SMM and estimate by bootstrap – see the previous section). Intuitively, the data induce little estimation error if W is small (the moments are precisely estimated). The second term comes from the noise we face when estimating the simulated moments: $\tilde{W}$ is the variance-covariance matrix of moments in simulated moments. It is an object that can also be estimated by bootstrap like W. Intuitively, the more precise the estimation of simulated moments (for instance, because the simulated dataset is very large), the smaller this term. Last, J is the Jacobian matrix around the SMM estimate. The bigger it is, the more sensitive moments are to parameters. And when this is the case, the estimation is more precise. With some abuse of language, economists tend to say that the model is well identified (locally, around $\hat{\Omega}$) when the coefficients in J are large. It is more accurate to say that the model is precisely estimated. We have a discussion like this in the main text (Section III) and report the log Jacobian matrix (the matrix of elasticities) in Table I.

Ideally, we would want to try to minimize the error coming from the imprecise

estimation of the model-generated moments. This estimation is imprecise because we do not simulate an infinitely large data set. If we did, we would have $\tilde{W} = 0$ and the second term in equation (IA5) would be zero. In Section II.B.3 of the Internet Appendix, we make sure that $\tilde{W}$ is as small as possible (by maximizing the number of observations and having one price path per firm), but, in practice, the sensitivity of investment to real estate prices is still estimated with significant error, which forces us not to neglect the second term in equation (IA5).

In practice, we compute W as described in Section II.B.2 of the Internet Appendix, and $\tilde{W}$ by bootstrapping the simulated sample using SMM-estimated parameters. We start with simulated data (100,000 firms followed over 100 years each). We then draw 100,000 firms from this sample *with replacement*. We compute the moments and repeat this procedure 100 times. Using these 100 sets of model-generated moments, we then compute the variance-covariance matrix $\tilde{W}$. We estimate J using the following technique. For each parameter j, we note $\hat{\Omega}_j$ the SMM estimate. We then simulate the model, holding the other parameters constant, for ω_j^+ immediately above $\hat{\omega}_j$ and ω_j^- immediately below. We use a 10-grid point scale as in Internet Appendix Figures IA1 to IA5. We compute model-generated moments m^+ and m^- associated with these two variants. The moment gradient $\frac{m^+ - m^-}{\omega_j^+ - \omega_j^-}$ is the j^{th} column of our estimate the J matrix.

III. Building the Data Set of Misspecification Errors

A. *Auxiliary Model*

We perform our Monte Carlo analysis using a dedicated and accelerated SMM procedure. This procedure relies on an auxiliary model that captures the relationships between each simulated moment and the vector of parameters $\Omega = (\rho, \sigma, s, c, e, h)$ estimated by the econometrician. Specifically, we assume that each moment k is a cubic polynomial function f_k of the parameters, including cross

terms. So the auxiliary model is a set of polynomial equations. Hence, if we know the coefficients of these polynomial functions, we can predict each simulated moment and the SMM error function using the auxiliary model. The advantage of this approach is that the computing time of the auxiliary model is shorter by several orders of magnitude.

The first step of this procedure is to train the auxiliary model. To do so, we generate a training sample using the real structural model. We draw 20,000 vectors of parameters Ω_i and generate the simulated moments $\widehat{m}(\Omega_i)$ by simulating the true structural model under our baseline specification and calibration. By doing so, we obtain a dataset with 20,000 observations, which contain the vector of generating parameters Ω_i and the vector of simulated moments $\widehat{m}(\Omega_i)$. The vectors Ω_i are drawn from a quasi-random (Halton) sequence with $\rho \in [0.50, 0.95]$, $\sigma \in [0.08, 0.17]$, $s \in [0.01, 1]$, $h \in [0.05, 0.4]$, $c \in [0, 0.04]$ and $e \in [0, 0.40]$.

Our goal is to use this training data set to predict the vector $\widehat{m}(\Omega_i)$ using polynomial approximations instead of the full structural model. We test this approach as follows.

1. Take a vector Ω_j and generate the vector of simulated moments $\widehat{m}(\Omega_j)$ using the full structural model.

2. Using the training data set, compute the SMM error function for each observation i, that is:

$$\left(\widehat{m}\left(\Omega_j\right) - \widehat{m}\left(\Omega_i\right)\right)' W \left(\widehat{m}\left(\Omega_j\right) - \widehat{m}\left(\Omega_i\right)\right)$$

3. For each moment k, estimate the generating funciton f_k with a weighted cubic polynomial regression, using the invert of the SMM error function as regression weights.

4. For each moment k, use the estimated polynomial $\hat{f}_k$ to predict the simulated moments $\hat{f}_k(\Omega_j)$.

By repeating this procedure 100 times, we get a sense of the quality of our auxiliary model. Specifically, we find that the auxiliary model predicts each simulated moment generated by the true structural model with an R^2 above 0.97. This out of sample performance gives us confidence that we can use this approach to perform our Monte Carlo analysis.

B. Monte Carlo Procedure

The Monte Carlo procedure works as follows. We start by drawing 4,000 vectors of parameters $\Omega_i = (\rho_i, \sigma_i, s_i, c_i, e_i, h_i)$ and six supplementary parameters $\Theta = (I_i, U_i, \sigma_{u,i}, \kappa_i, d_{0,i}, \tau_i)$. To do so, we use a quasi-random (Halton) sequence with $\rho \in [0.80, 0.95]$, $\sigma \in [0.10, 0.15]$, $s \in [0.10, 0.7]$, $h \in [0.10, 0.3]$, $c \in [0, 0.03]$, $e \in [0, 0.30]$, $I \in [0, 0.4]$, $U \in [0, 0.4]$, $\kappa \in [-0.3, 0.3]$, $d_0 \in [0, 0.4]$, $\sigma_u \in [0, 0.03]$ and $\tau \in [1/3 - 0.075, 1/3 + 0.075]$.

Next, for each random draw, we follow the steps below.

1. Solve the true, correctly specified model and simulate the moments. Compute the true TFP and output losses caused by financial constraints.

2. Set $\Theta = (0, 0, 0, 0, 0, 0.33)$ as in our baseline specification and estimate the vector Ω by SMM. First, we target our investment sensitivity moment. Because we need to estimate the model thousands of times, we use the auxiliary model described in Section III.A of the Internet Appendix and the global optimization routine described in Section II.B.4 of the Internet Appendix.

3. Compute the TFP losses and output losses implied by the structural estimation of the misspecified model.

4. Repeat the last two steps but target leverage instead of the investment sensitivity moment.

IV. Detailed Description and Robustness of Table V of the Main Article

First, we explain in detail the adjustments we make to calculate leverage and estimate β under the various sources of misspecification considered in Table V of the main article. Line 1 corresponds to our baseline estimate for β and our baseline leverage.

In line 2, debt is unchanged but total assets are now the sum of book assets and the off-balance-sheet intangible capital in Peters and Taylor (2017). For the estimation of β, the dependent variable is the ratio of capital expenditures plus R&D expenditures plus 30% of SG&A (Peters and Taylor (2017)), normalized by the sum of lagged tangible assets and lagged intangible capital ($k^{\text{intangible}}$ from Peters and Taylor (2017)). In terms of explanatory variables, $REValue_{it}$ is normalized by lagged tangible assets and lagged intangible capital ($k^{\text{intangible}}$ from Peters and Taylor (2017)); cash flows add back $(1-\tau)$ of the expenditures in intangible capital (capital expenditures plus R&D expenditures plus 30%) and are normalized by lagged tangible assets and lagged intangible capital (Peters and Taylor (2017)). We use a tax rate of $\tau = 30\%$. We use the total Q in Peters and Taylor (2017) as our measure of Q.

In line 3, we calculate leverage by adding leases to both the numerator and the denominator of our baseline measure. We calculate leases following an approach similar to Rampini and Eisfeldt (2009). For each firm-year, we compute l, the ratio of operating lease rentals (lagged COMPUSTAT item mrc1) to on-balance sheet capital rental (depreciation plus 10% of total assets (COMPUSTAT item at)). We then compute leases as $l \times at$. To estimate β, the dependent variable is the ratio of capital expenditures plus the yearly difference in leases, normalized by the sum of lagged tangible assets and lagged leases. In terms of explanatory variables, $REValue_{it}$ and cashflows are normalized by the sum of lagged tangible assets and lagged leases. Our market-to-book ratio is similar to the baseline, except that the denominator is now the sum of total assets and leases.

In line 4, we calculate leverage by adding the present value of lease commitments (PV(lease)) to the net debt used in our baseline measure. To calculate PV(lease), we start from the next five years commitments (mtr1-5), spread expected commitment (mrtca) over these five years equally, and calculate the present value of these commitments at a 10% discount rate. The estimate for β corresponds to the baseline estimate since the measurement of capital is similar to the baseline.

In line 5, we calculate leverage by adding account payables (ap) to the net debt used in our baseline measure. To estimate β, the dependent variable is now the ratio of capital expenditures plus the yearly difference in current assets, normalized by the sum of lagged tangible assets and lagged current assets. $REValue_{it}$ and cash-flows are normalized by the sum of lagged tangible assets and lagged current assets. Our market-to-book ratio is similar to the baseline.

In line 6, we calculate leverage by using the economic value of the physical capital stock instead of net PPE in the denominator. To calculate the capital stock, we start with net PPE (COMPUSTAT item ppent) in the first year the firm appears in COMPUSTAT (or in 1981 if the firm appears prior to 1981). Every year, we then add capital expenditures (COMPUSTAT item capx), subtract sale of property (COMPUSTAT item sppe) and depreciate the previous year capital stock at a 6% rate, which is typical in the macro-finance literature (e.g., Midrigan and Xu (2014)). Leverage is then calculated as the ratio of net debt to total assets minus PPE plus the physical capital stock. To estimate β, the dependent variable is the ratio of capital expenditures normalized by the lagged physical capital stock, $REValue_{it}$, and cashflows are normalized by the lagged capital stock. The market-to-book ratio is similar to the baseline, except that the denominator is total assets minus net PPE plus the capital stock calculated with the inventory method.

In line 7, we combine all these adjustments. We calculate net debt using the baseline measure, to which we add leases and accounts payables. Total assets are given by assets minus PPE plus the physical capital stock, to which we add leases, and the off-balance-sheet part of intangible capital ($K_{int}^{\text{off b-s}}$). Leverage is the ratio

of these two variables. To estimate β, we use the following dependent variable:

$$Y_t = \frac{capital\ expenditures_t + R\&D\ expenditures_t + 30\%\ SG\&A_t + (leases_t - leases_{t-1}) + (Current_t - Current_{t-1})}{K_{t-1} + current_{t-1} + leases_{t-1} + k_{t-1}^{intangible}}, \quad \text{(IA5)}$$

where K_{t-1} corresponds to the lagged capital stock calculated using the perpetual inventory methodology described above, and $REValue_{it}$ and cashflows are normalized by the same denominator as that in Y_t. As in line 2, cashflows include (1-τ)($R\&D\ expenditures_t + 30\%\ SG\&A_t$). Finally, our measure of Q is as in the baseline, but the denominator is ($total\ assets + capital\ stock - PPE + leases + k_{int}^{off\ bs} + current$), where $k_{int}^{off\ bs}$ is the off-balance-sheet intangible capital from Peters and Taylor (2017).

All of these statistics are computed using equal weighting. Equally weighted statistics are natural counterparts to our model-generated moments, since firms in our model are ex ante identical – they all have the same data generating process – so there is no obvious reason to match size-weighted moments. Another advantage of equally weighted statistics is that they are less noisy: since firm size distribution is very concentrated at the top, size weighting gives a disproportionate weight to a few large firms, rendering estimates noisy.

These caveats notwithstanding, a natural question is whether our estimates in Table V of the main article are robust to size weighting, as the largest firms matter disproportionately for the macroeconomy. We show these results in Internet Appendix Table IAII. As expected given the skewness of firm size distribution, estimated moments are a bit more volatile, but the orders of magnitude obtained are very similar to our main estimates.

Table IAI
Effect of Real Estate Value on Investment Controlling for City-Year Dummies

In this table, we regress the investment rate on a measure of real estate value and a series of controls. Real estate value is essentially the interaction between firms' real estate ownership at book value and MSA-level office price inflation. We use the baseline specification and data set of Chaney, Sraer, and Thesmar (2012) in column (1). In column (2), we add MSA dummies interacted with year dummies. In both specifications, controls interacted with office prices are quintiles of age, ROA, assets, as well as industry and state dummies. All regressions are clustered at the firm level. *** indicates significant at the 1% level.

	Investment / Assets	
	(1)	(2)
Real Estate Value	0.062***	0.06***
	(0.0069)	(0.007)
Cash Flow	0.026***	0.026***
	(0.0035)	(0.0035)
Q	0.07***	0.068***
	(0.0038)	(0.0039)
Observations	17,458	17,440
R^2	0.42	0.44
Controls $\times$ prices	Yes	Yes
Year FE	Yes	Yes
Firm FE	Yes	Yes
MSA-year FE	No	Yes

Table IAII
Asset-Weighted Leverage Ratios and β Using Alternative Definition

Same construction as in Table V of the main article, except that all means and regression coefficients are weighted by one plus lagged total assets (lagged by one year).

	Definition	D	Assets	K	I	Leverage =D/Assets	β
1	Standard	dltt+dlc-che	at	ppent	capx	0.203 (0.026)	0.023 (0.015)
2	Intangible	dltt+dlc-che	at+$k_{\text{int}}^{\text{off-bs}}$	ppent+k_{int}	capx +xrd+.3$\times$xsga	0.169 (0.024)	0.034 (0.014)
3	Leasing 1	dltt+dlc-che +lease	at+lease	ppent+lease +lease-lease(t-1)	capx	0.251 (0.024)	0.008 (0.014)
4	Leasing 2	dltt+dlc-che +PV(lease)	at	ppent	capx	0.167 (0.029)	0.023 (0.015)
5	Account payables	dltt+dlc-che +ap	at	ppent+act	capx+act-act(t-1)	0.285 (0.027)	0.027 (0.017)
6	Real depreciation	dltt+dlc-che	at+K-ppent	K	capx	0.183 (0.021)	0.138 (0.045)
7	All adjustments	dltt+dlc-che +lease+ap	at+K-ppent +lease+$k_{\text{int}}^{\text{off-bs}}$	ppent+k_{int} +lease+act	capx+act-act(t-1) +lease-lease(t-1) +(1-τ)(xrd+.3$\times$xsga)	0.243 (0.019)	0.042 (0.021)

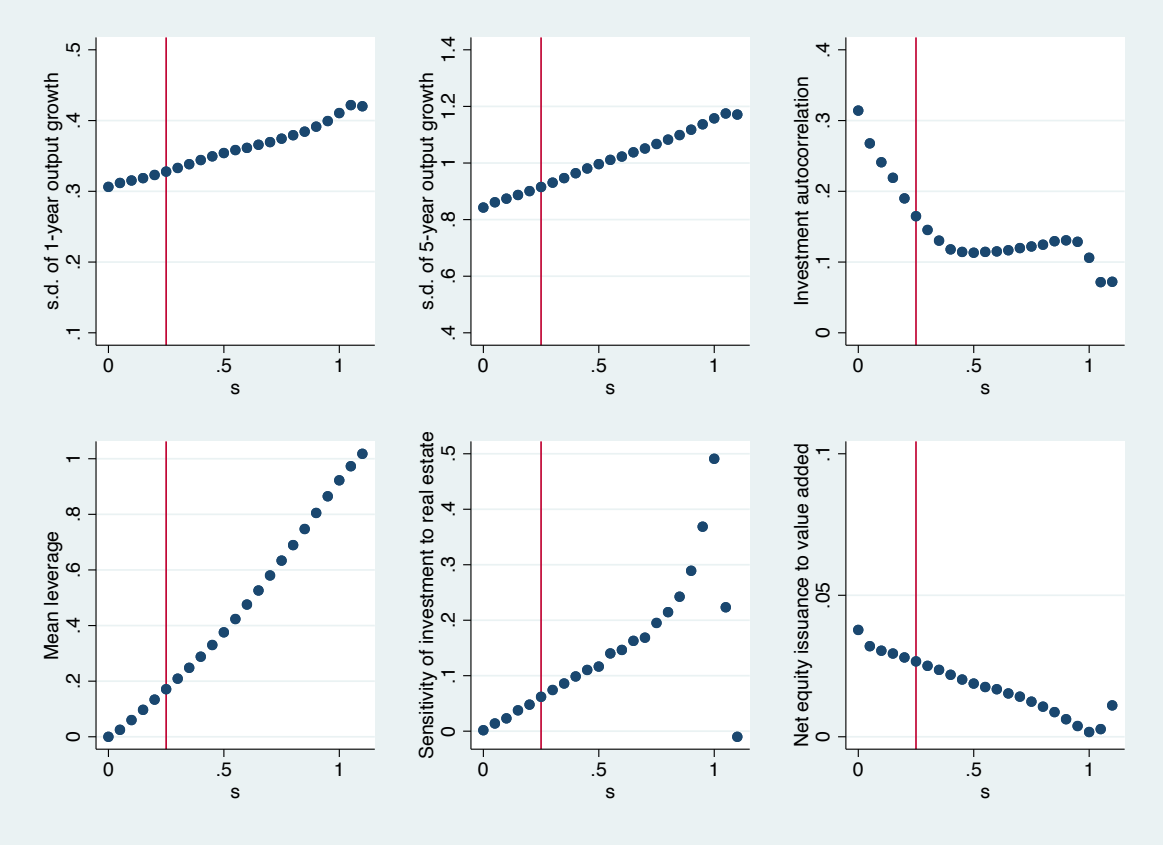

Figure IA1. Sensitivity of moments to pledgeability s. In this figure, we set all of the estimated parameters (s, c, ρ, σ, H and e) at their SMM estimate in our preferred specification – as per column (3), Panel A in Table II of the main article. We fix w and Q at their reference levels: $w = 0.03$ and $Q = 1$. We then vary s from zero to one. For each value of s that we choose, we solve the model, simulate the data, and compute four target moments, plus the average leverage ratio and the sensitivity of debt issuance to real estate value. Each panel corresponds to one moment. The red vertical line corresponds to the SMM estimate of s.

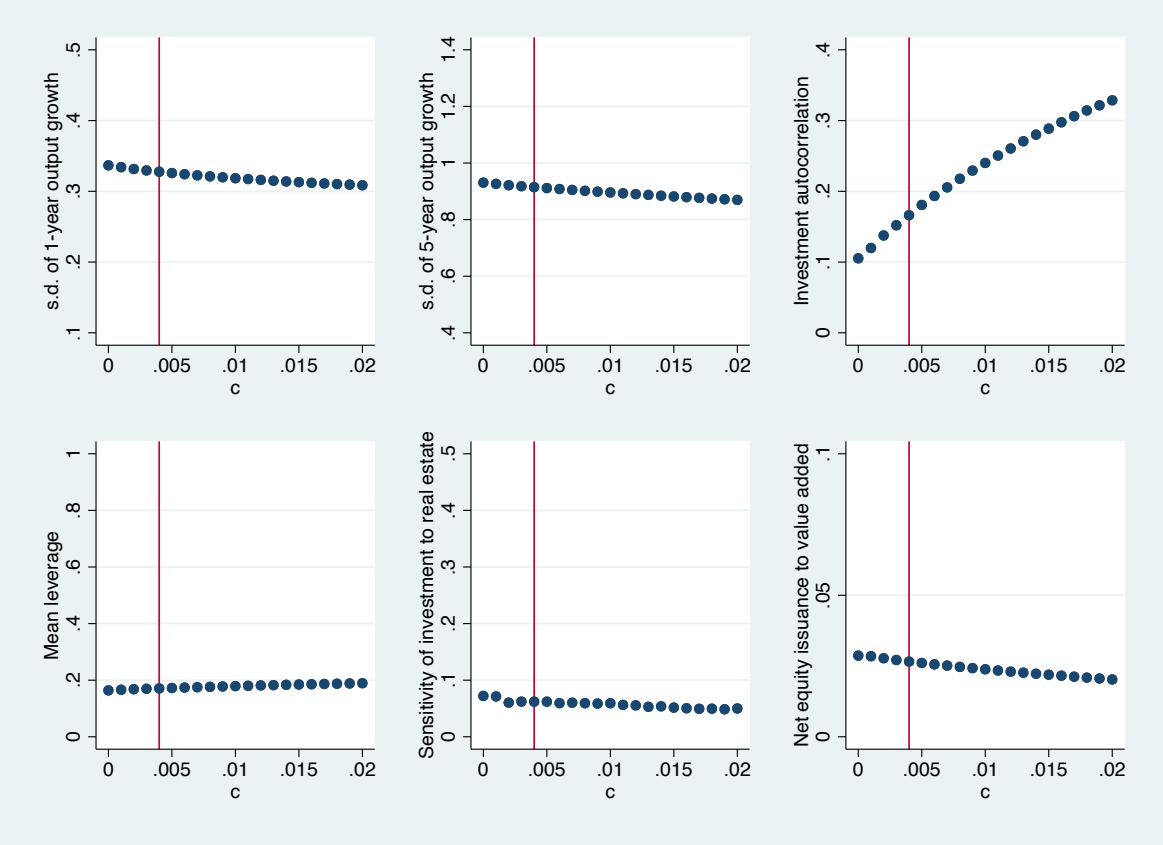

Figure IA2. Sensitivity of moments to pledgeability c. In this figure, we set all of the estimated parameters (s, c, ρ, σ, H and e) at their SMM estimate in our preferred specification – as per column (3), Panel A in Table II of the main article. We fix w and Q at their reference levels: $w = 0.03$ and $Q = 1$. We then vary c from zero to 0.02. For each value of c that we choose, we solve the model, simulate the data, and compute four target moments, plus the average leverage ratio and the sensitivity of debt issuance to real estate value. Each panel corresponds to one moment. The red vertical line corresponds to the SMM estimate of c.

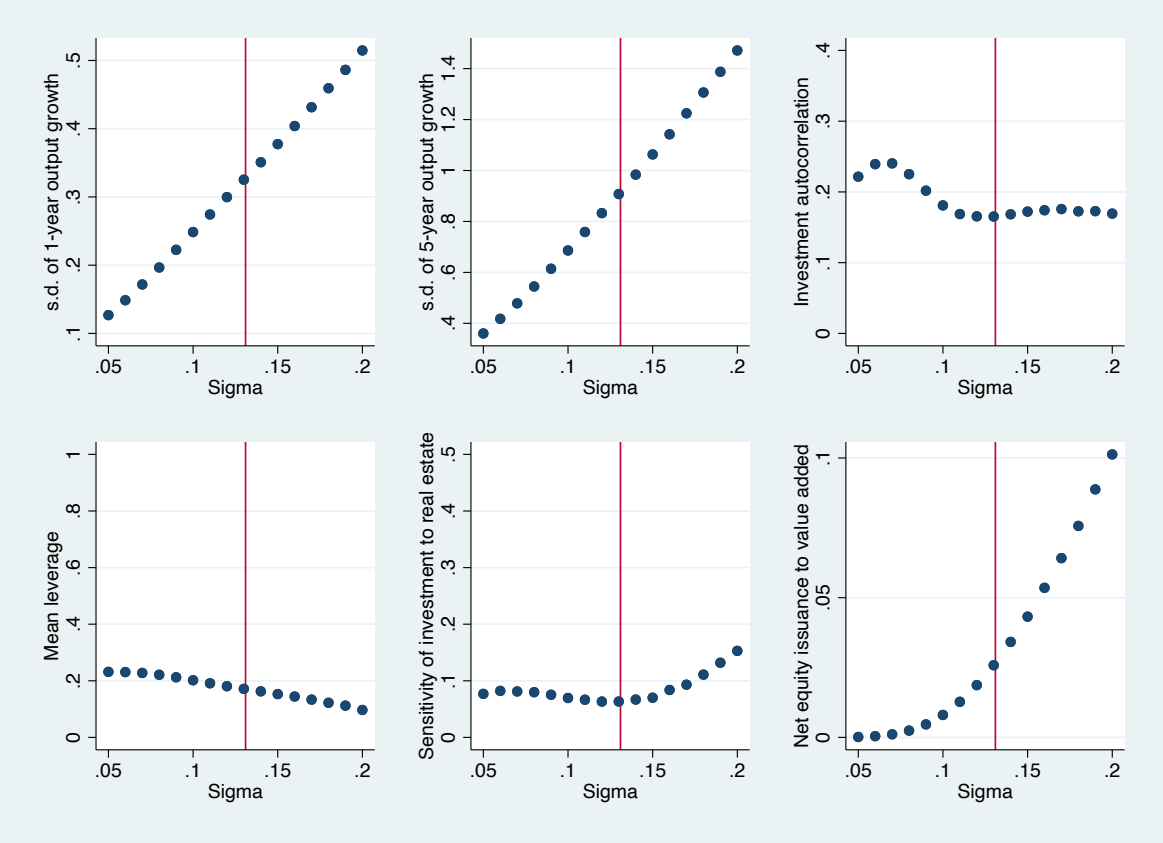

Figure IA3. Sensitivity of moments to pledgeability σ. In this figure, we set all of the estimated parameters (s, c, ρ, σ, H and e) at their SMM estimate in our preferred specification – as per column (3), Panel A in Table II of the main article. We fix w and Q at their reference levels: $w = 0.03$ and $Q = 1$. We then vary σ from zero to 0.2. For each value of σ that we choose, we solve the model, simulate the data, and compute four target moments, plus the average leverage ratio and the sensitivity of debt issuance to real estate value. Each panel corresponds to one moment. The red vertical line corresponds to the SMM estimate of σ.

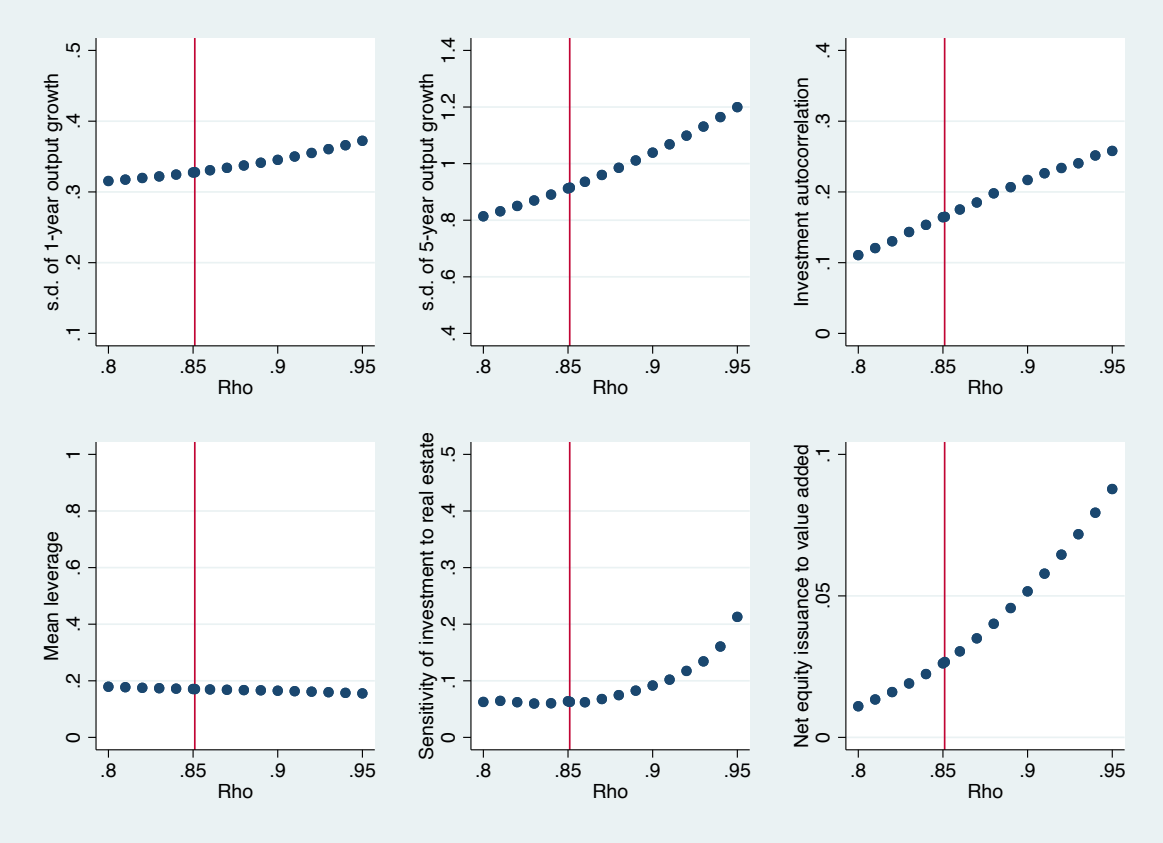

Figure IA4. Sensitivity of moments to pledgeability ρ. In this figure, we set all of the estimated parameters (s, c, ρ, σ, H and e) at their SMM estimate in our preferred specification – as per column (3), Panel A in Table II of the main article. We fix w and Q at their reference levels: $w = 0.03$ and $Q = 1$. We then vary ρ from 0.8 to 0.95. For each value of ρ that we choose, we solve the model, simulate the data, and compute four target moments, plus the average leverage ratio and the sensitivity of debt issuance to real estate value. Each panel corresponds to one moment. The red vertical line corresponds to the SMM estimate of ρ.

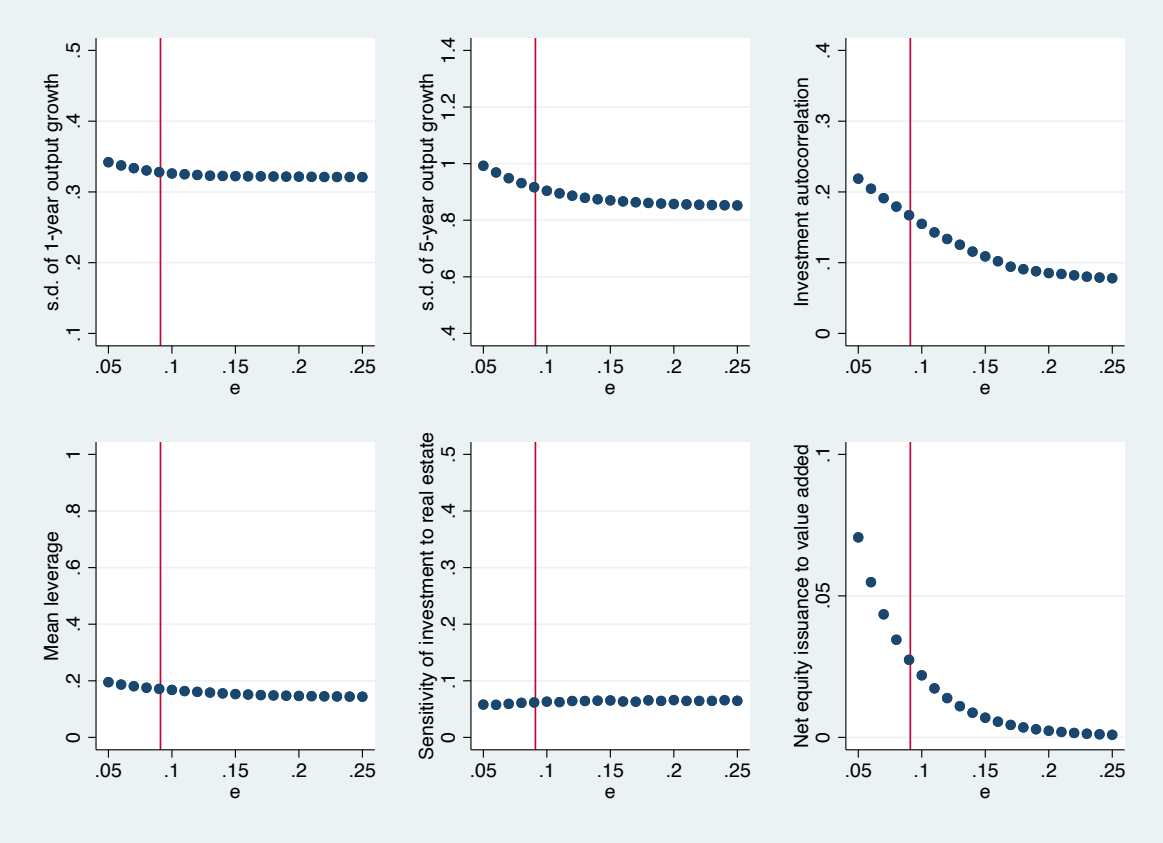

Figure IA5. Sensitivity of moments to pledgeability e. In this figure, we set all of the estimated parameters (s, c, ρ, σ, H and e) at their SMM estimate in our preferred specification – as per column (3), Panel A in Table II of the main article. We fix w and Q at their reference levels: $w = 0.03$ and $Q = 1$. We then vary e from 0.05 to 0.25. For each value of e that we choose, we solve the model, simulate the data, and compute four target moments, plus the average leverage ratio and the sensitivity of debt issuance to real estate value. Each panel corresponds to one moment. The red vertical line corresponds to the SMM estimate of e.

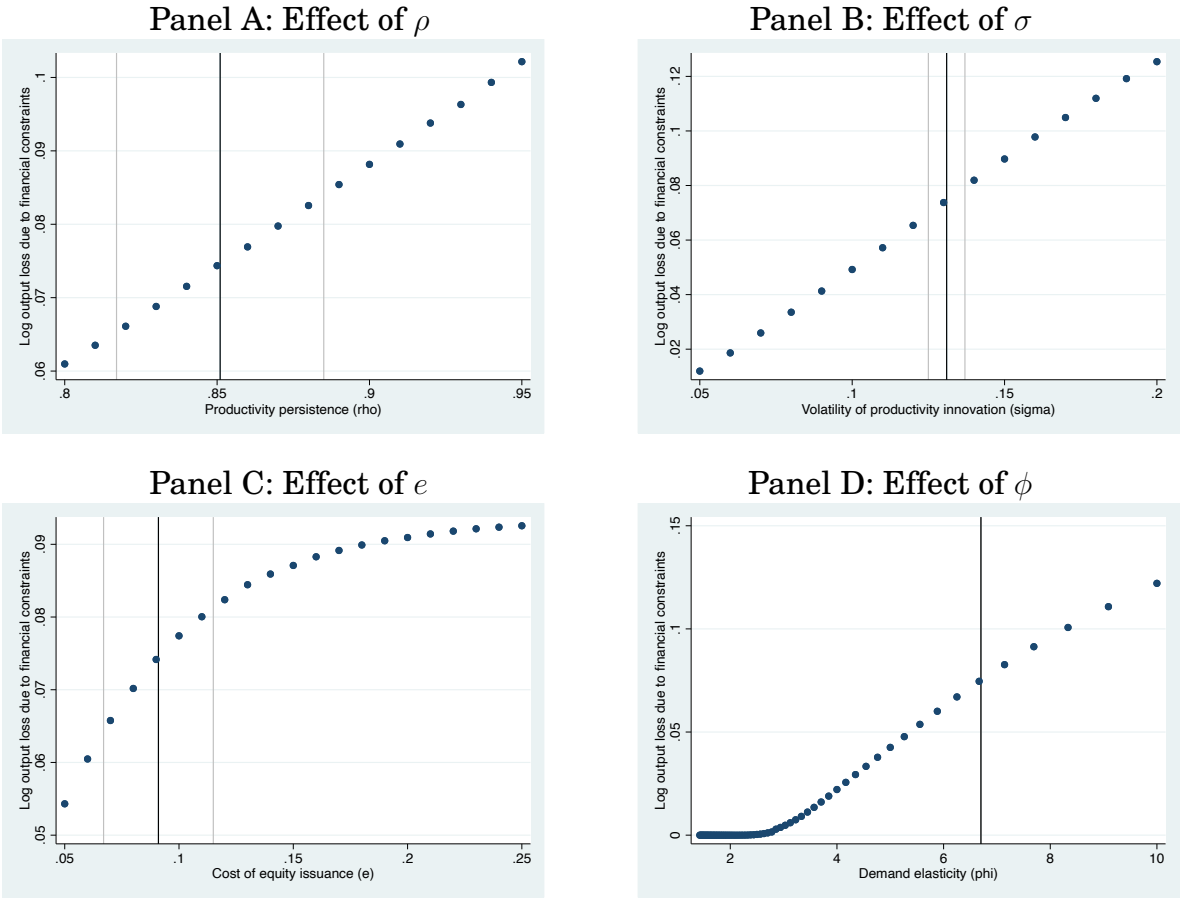

Figure IA6. Aggregate output: Additional comparative statics. This figure reports the effect of changing various parameters on the output loss of financing constraints. We vary productivity persistence in Panel A (ρ), productivity innovation volatility in Panel B (σ), equity issuance costs in Panel C (e), and price elasticity ϕ in Panel D. In Panels A, B, and C, the vertical black line correspond to the SMM estimates and the grey lines the borders of the 90% confidence interval. In Panel D, we do not report confidence intervals because ϕ is calibrated, not estimated. The values we span correspond to the range of values in Broda and Weinstein (2006).

Panel A: Share of intangible > 0

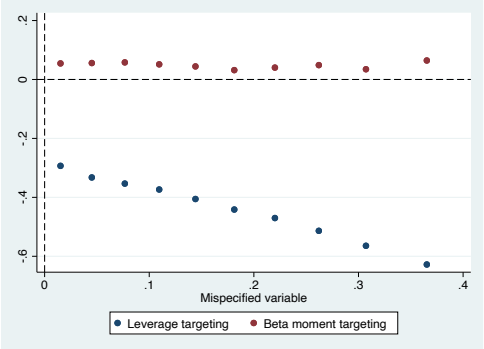

Panel B: Unaccounted capital > 0

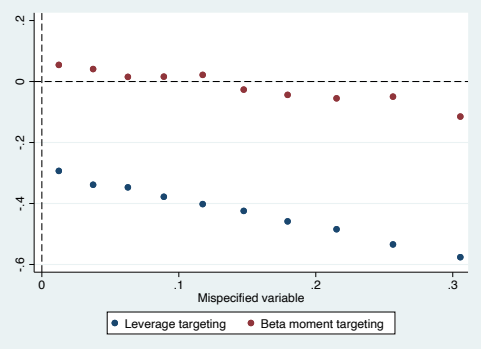

Panel C: Real estate price noise > 0

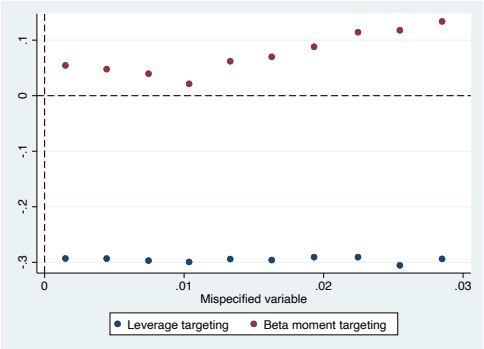

Panel D: Unobserved debt need/capacity $\neq 0$

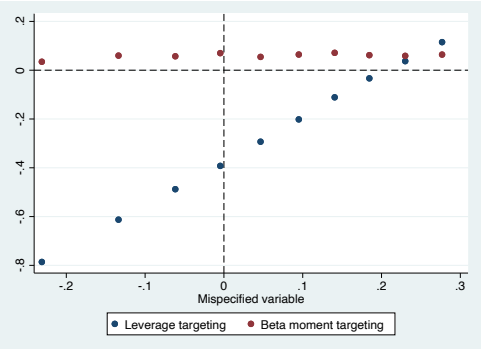

Panel E: Unsecured debt capacity > 0

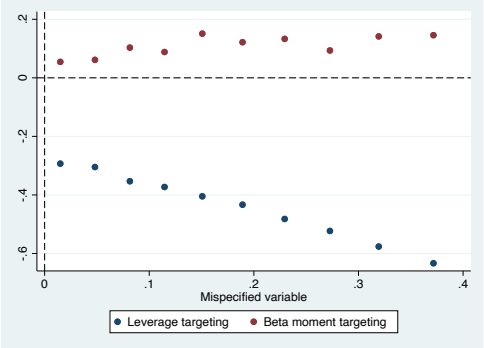

Panel F: True tax rate $\neq 33\%$

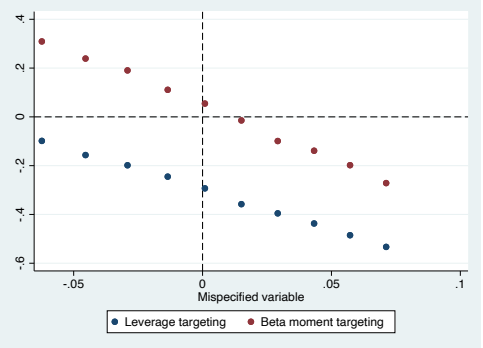

Figure IA7. Misspecification and TFP loss estimation error, leverage vs β targeting. In this figure, we report the effect of misspecification on the estimation of TFP loss. Each panel is a form of "controlled binscatter." On our sample of 4,000 simulations, we first regress misspecification errors (relative to the true loss) on decile dummies for the six parameters governing misspecification (Θ), taking the first decile as reference. We do this for the two sets of misspecification errors obtained using either inference based on leverage (blue dots) or inference based on the reduced-form coefficient β (red dots). For each parameter, we then plot the predicted value for each decile against the average value of the parameter for this decile while setting the other parameters to their average values.

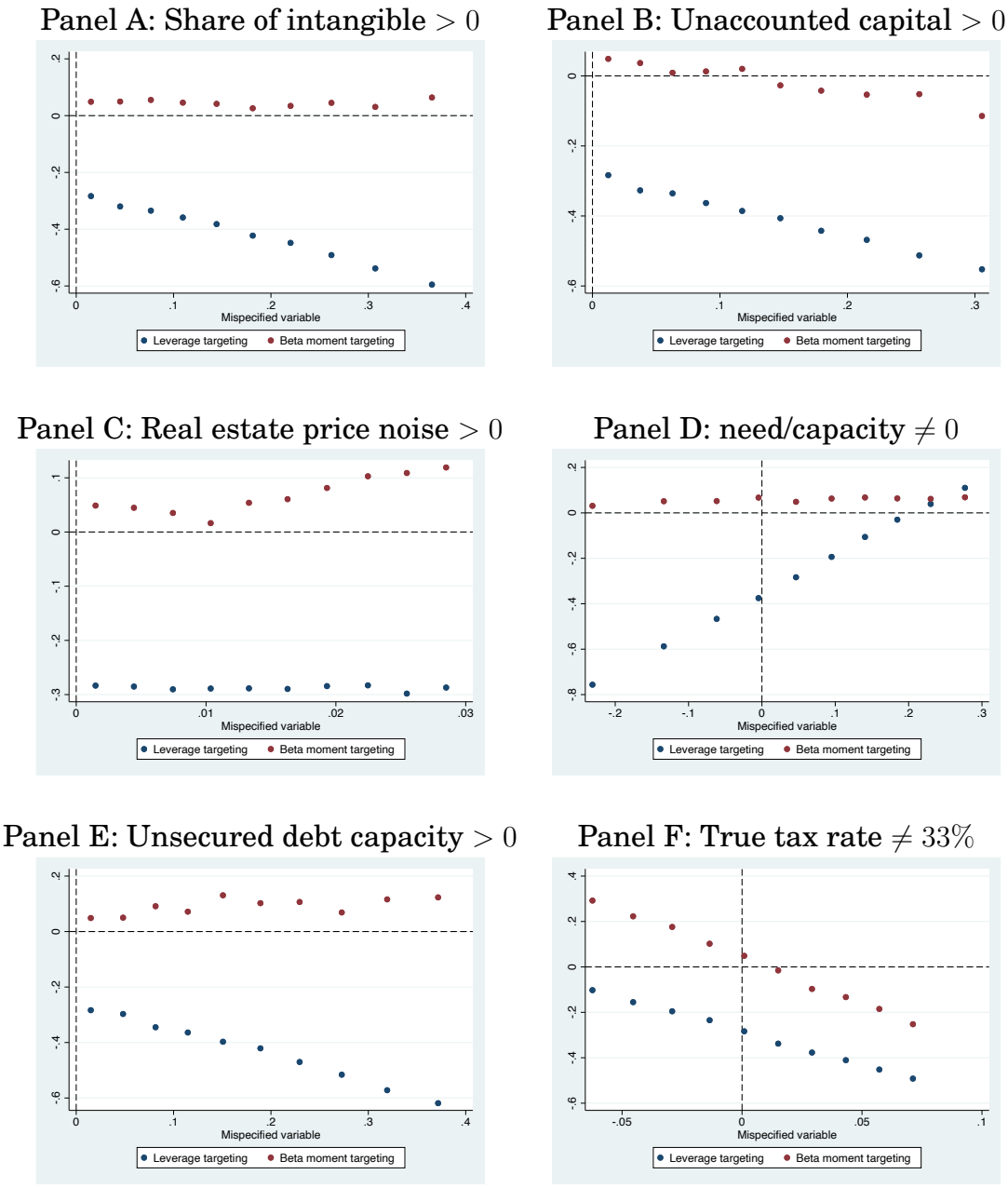

Figure IA8. Misspecification and output loss estimation error, leverage vs β targeting. In this figure, we report the effect of misspecification on the estimation of output loss. Each panel is a form of "controlled binscatter." On our sample of 4,000 simulations, we first regress misspecification errors (relative to the true loss) on decile dummies for the six parameters governing misspecification (Θ), taking the first decile as reference. We do this for the two sets of misspecification errors obtained using inference based on leverage (blue dots) or inference based on the reduced-form coefficient β (red dots). For each parameter, we then plot the predicted value for each decile, against the average value of the parameter for this decile, while setting the other parameters to their average values.

References

Amaral, Pedro S., and Erwan Quintin, 2010, Limited enforcement, financial intermediation, and economic development: A quantitative assessment, *International Economic Review* 51, 785–811.

Arellano, Cristina, Yan Bai, and Jing Zhang, 2012, Firm dynamics and financial development, *Journal of Monetary Economics* 59, 533–549.

Begenau, Juliane, and Juliana Salomao, 2018, Firm financing over the business cycle, *Review of Financial Studies* 32, 1235–1274.

Bernanke, Ben S., Mark Gertler, and Simon Gilchrist, 1999, The financial accelerator in a quantitative business cycle framework, in John B Taylor, Michael Woodford, and Harald Uhlig, eds., *Handbook of Macroeconomics*, 1341–1393 (Elsevier).

Broda, Christian, and David Weinstein, 2006, Globalization and the gains from variety, *Quarterly Journal of Economics* 121, 541–585.

Buera, Francisco J., and Yongseok Shin, 2013, Financial frictions and the persistence of history: A quantitative exploration, *Journal of Political Economy* 121, 221–272.

Chaney, Thomas, David Sraer, and David Thesmar, 2012, The collateral channel: How real estate shocks affect corporate investment, *American Economic Review* 102, 2381–2409.

Cooley, Thomas F., and Vincenzo Quadrini, 2001, Financial markets and firm dynamics, *American Economic Review* 91, 1286–1310.

DeAngelo, Harry, Linda DeAngelo, and Toni M. Whited, 2011, Capital structure dynamics and transitory debt, *Journal of Financial Economics* 99, 235–261.

Garcia-Macia, Daniel, 2017, The financing of ideas and the great deviation, Working Paper 2017/176, International Monetary Fund.

Gilchrist, Simon, Jae W. Sim, and Egon Zakrajšek, 2014, Uncertainty, financial frictions, and investment dynamics, Working Paper 20038, National Bureau of Economic Research.

Gomes, Joao F., and Lukas Schmid, 2010, Levered returns, *The Journal of Finance* 65, 467–494.

Gopinath, Gita, Şebnem Kalemli-Özcan, Loukas Karabarbounis, and Carolina Villegas-Sanchez, 2017, Capital allocation and productivity in south europe, *Quarterly Journal of Economics* 132, 1915–1967.

Greenwood, Jeremy, Juan M. Sanchez, and Cheng Wang, 2013, Quantifying the impact of financial development on economic development, *Review of Economic Dynamics* 16, 194–215, Special issue: Misallocation and Productivity.

Guvenen, Faith, Serdar Ozkan, and Jae Song, 2014, The nature of countercyclical income risk, *Journal of Political Economy* 122, 612.

Hall, Bronwyn H., Robert E. Hall, John Heaton, and N. Gregory Mankiw, 1993, The value and

performance of U.S. corporations, *Brookings Papers on Economic Activity* 1993, 1–49.

Hennessy, Christopher, and Toni Whited, 2005, Debt dynamics, *The Journal of Finance* 60, 1129–1165.

Hennessy, Christopher, and Toni Whited, 2007, How costly is external financing? Evidence from a structural estimation, *Journal of Finance* 62, 1705–1745.

Itskhoki, Oleg, and Benjamin Moll, 2019, Optimal development policies with financial frictions, *Econometrica* 87, 139–173.

Jermann, Urban, and Vincenzo Quadrini, 2012, Macroeconomic effects of financial shocks, *American Economic Review* 102, 238–271.

Jo, In Hwan, and Tatsuro Senga, 2019, Aggregate consequences of credit subsidy policies: Firm dynamics and misallocation, *Review of Economic Dynamics* 32, 68–93.

Kahn, Aubik, and Julia Thomas, 2013, Credit shocks and aggregate fluctuations in an economy with production heterogeneity, *Journal of Political Economy* 121, 1055–1107.

Li, Shaojin, Toni M. Whited, and Yufeng Wu, 2016, Collateral, taxes, and leverage, *Review of Financial Studies* 29, 1453–1500.

Liu, Zheng, Pengfei Wang, and Tao Zha, 2013, Land-price dynamics and macroeconomic fluctuations, *Econometrica* 81, 1147–1184.

Michaels, Ryan, Page T. Beau, and Toni M. Whited, 2018, Labor and capital dynamics under financing frictions, *Review of Finance* 23, 279–323.

Midrigan, Virgiliu, and Daniel Yi Xu, 2014, Finance and misallocation: Evidence from plant-level data, *American Economic Review* 104, 422–58.

Moll, Benjamin, 2014, Productivity losses from financial frictions: Can self-financing undo capital misallocation?, *American Economic Review* 104, 3186–3221.

Nikolov, Boris, Lukas Schmid, and Roberto Steri, 2019, Dynamic corporate liquidity, *Journal of Financial Economics* 132, 76–102.

Ottonello, Pablo, and Thomas Winberry, 2020, Financial heterogeneity and the investment channel of monetary policy, *Econometrica* 88, 2473–2502.

Peters, Ryan, and Lucian Taylor, 2017, Intangible capital and the investment-q relation, *Journal of Financial Economics* 123, 251–272.

Rampini, Adriano, and Andrea Eisfeldt, 2009, Leasing, ability to repossess, and debt capacity, *Review of Financial Studies* 22, 1621–1657.